International Journal of Thermophysics, Vol. 19, No. 1, 1998

Explicit Corrections for the Effect of Viscous Heating in Circular Couette Viscometers

T. D. Papathanasiou[1]

Received October 20, 1997

Based on asymptotic solutions to the problem of coupled flow and heat transfer in circular Couette flow of materials whose viscosity and thermal conductivity are polynomial functions of temperature, we obtain expressions for the effect of viscous heating on the gapwise distribution of shear rate under isothermal and adiabatic wall conditions. These expressions are shown to exhibit the anticipated asymptotic behavior as the gap-to-diameter ratio approaches unity and are in agreement with numerical results for a reasonable range of the Nahme number. Following that, we derive explicit rheological corrections for circular Couette–Hatschek viscometers; these account for the effect of viscous heating in the presence of temperature-dependent fluid properties and are reliable for values of the correction factor down to around 0.8.

KEY WORDS: Couette viscometer; rheology; rheological corrections; viscous heating.

1. INTRODUCTION

When viscous materials undergo shear flow, energy is dissipated due to internal friction. When the ratio of the amount of generated heat to the amount of heat removed from the material through conduction (that is, the Brinkman number) is not negligible, a nonisothermal temperature profile establishes itself in the sheared fluid. When the fluid viscosity is in turn a function of temperature (as is the case in almost all fluids of practical interest), the kinematics of the flow are affected by this nonuniform temperature field. This *thermomechanical coupling* can give rise to significant deviations

[1] Department of Chemical Engineering, Swearingen Engineering Center, University of South Carolina, Columbia, South Carolina 29208, U.S.A.

0195-928X/00/0700-0071$18.00/0

from the anticipated velocity profiles and can be the source of significant errors in viscometric measurements at high shear rates, particularly with rotational viscometers in which the entire sample is continuously sheared during the measurement.

Utilizing a proposed method [1, 2], we have presented [3] asymptotic solutions for the temperature and velocity profiles in planar Couette flow of a fluid whose viscosity and thermal conductivity are polynomial functions of temperature. Based on these, we derived formal corrections, up to fourth order in the Brinkman number, for viscometric measurements in a narrow-gap Couette. Furthermore, we have extended this approach and have derived similar asymptotic solutions for the effect of viscous heating on the velocity and temperature profiles in the case of circular Couette flow (again, with viscosity and thermal conductivity described as quadratic functions of temperature [4]). This device has recently received increased attention as suitable for the study of microstructure evolution during processing of concentrated suspensions [5–7] as well as in the study of fiber motion in nonhomogeneous flow fields. Based on these results for the velocity profile, the present communication derives and tests expressions for the distribution of shear rate in circular Couette flow under conditions of isothermal and adiabatic walls. From these, we derive formal corrections for the effect of viscous heating in Couette viscometers of nonnegligible eccentricity.

2. MODEL EQUATIONS

We consider steady, incompressible flow in the Couette device shown in Fig. 1. This device consists of two concentric cylinders of radii R and κR ($\kappa < 1$), of which the inner one is stationary and the outer is rotating with constant angular velocity Ω. The only nonzero velocity component in this geometry is the tangential velocity u_θ, there is no tangential pressure drop and the equations of motion and energy reduce to

$$\frac{1}{x^2}\left\{\frac{\partial}{\partial x}\left\{\frac{\mu}{\mu_0}x^3\frac{\partial}{\partial x}\left(\frac{u}{x}\right)\right\}\right\}=0 \tag{1}$$

$$\frac{1}{x}\frac{\partial}{\partial x}\left\{\frac{k}{k_0}x\frac{\partial \Theta}{\partial x}\right\}+\mathrm{Br}\,\frac{\mu}{\mu_0}\left[x\frac{\partial}{\partial x}\left(\frac{u}{x}\right)\right]^2=0 \tag{2}$$

where the following nondimensionalization has been applied:

$$\Theta=\frac{T-T_0}{T_0},\qquad x=\frac{r}{R},\qquad u=\frac{u_\theta}{\Omega R},\qquad \mathrm{Br}=\frac{\mu_0(\Omega R)^2}{k_0 T_0} \tag{3}$$

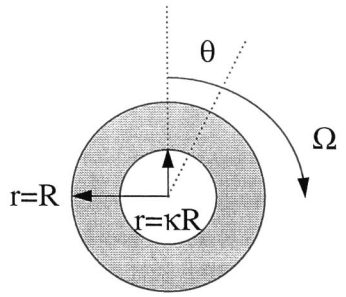

Fig. 1. Schematic diagram of the Couette apparatus.

It should be pointed out that this representation does not consider deviations in flow due to the finite height of the viscometer and thus, end effects are not dealt with in the present study. In Eq. (3), Br is the Brinkman number, which is a measure of the heat generated by viscous heating compared to the heat conducted through the material, and T_0 is a reference temperature. Closed-form solutions to Eqs. (1) and (2) have been obtained for certain limiting cases (Refs. 1, 2, 8, 9 and references therein). When the fluid viscosity and thermal conductivity can be expressed as general polynomial functions of temperature,

$$\frac{k}{k_0} = 1 + \sum_{i=1}^{I} \alpha_i \Theta^i \tag{4}$$

$$\frac{\mu_0}{\mu} = 1 + \sum_{i=1}^{I} \beta_i \Theta^i \tag{5}$$

where the subscript (0) indicates (known) property values corresponding to a reference temperature, series solutions to Eqs. (1) and (2) can be formulated as perturbations with respect to the Brinkman number [1, 2, 8]:

$$\frac{u(x)}{x} = u_0(x) + \sum_{n=1}^{N} u_n(x)\,\mathrm{Br}^n \tag{6}$$

$$\Theta(x) = \Theta_0(x) + \sum_{n=1}^{N} \Theta_n(x)\,\mathrm{Br}^n \tag{7}$$

A procedure for obtaining the coefficient functions $u_0(x) - u_N(x)$ and $\Theta_1(x) - \Theta_N(x)$ for planar Couette flow has been outlined in Refs. 1 and 2 and has been applied in the case of circular Couette flow in Ref. 4. We are

interested here in the use of these results to obtain the distribution of shear rate across the gap of the Couette and, from that, obtain rheological corrections accounting for the effect of viscous heating in circular Couette flow. We consider the following boundary conditions.

Case I (*isothermal walls at* x = 1 *and* x = κ):

$$x=\kappa \quad \text{(inner cylinder):} \quad u=0 \quad \text{and} \quad \Theta=0 \tag{8a}$$

$$x=1 \quad \text{(outer cylinder):} \quad u=1 \quad \text{and} \quad \Theta=0 \tag{8b}$$

Case II (*isothermal walls at* x = 1 *and adiabatic wall at* x = κ):

$$x=\kappa \quad \text{(inner cylinder):} \quad u=0 \quad \text{and} \quad (d\Theta/dx)=0 \tag{9a}$$

$$x=1 \quad \text{(outer cylinder):} \quad u=1 \quad \text{and} \quad \Theta=0 \tag{9b}$$

2.1. Series Solution for $\gamma_{r\theta}(x)$

The sought expressions for the shear rate $[\gamma_{r\theta}(x)]$ across the gap will come in a form similar to that of Eqs. (6) and (7), namely,

$$\gamma_{r\theta}(x)=x[\gamma_0(x)+\mathrm{Br}\,\gamma_1(x)+\mathrm{Br}^2\gamma_2(x)] \tag{10}$$

It should be pointed out that expansion of $\gamma(x)$ to second order in Br requires expansions of k/k_0 to first order and of μ_0/μ to second order in Θ. The coefficients $\gamma_0(x)-\gamma_2(x)$ for Case I and Case II are obtained by differentiating the velocity profile of Eq. (6) [4], according to the definition

$$\gamma_{r\theta}=x\frac{\partial}{\partial x}\left(\frac{u(x)}{x}\right) \tag{11}$$

These coefficients are as follows.

Case I:

$$\gamma_0(x)=\frac{C_0}{x^3}, \qquad \text{where} \quad C_0=\frac{2\kappa^2}{1-\kappa^2} \tag{12}$$

$$\gamma_1(x):=\frac{\beta_1\kappa^4}{\ln(\kappa)(\kappa^2-1)^3}\left[\frac{(-\ln(\kappa)\kappa^2+2\ln(x)\kappa^2+\ln(\kappa)-2\ln(x)+1-\kappa^2)}{x^3}\right.$$

$$\left.+2\ln(\kappa)\frac{\kappa^2}{x^5}\right] \tag{13}$$

$$\gamma_2(x) := \frac{1}{24(\kappa^2-1)^5 \ln(\kappa)^2}\left[\Gamma_\alpha \frac{1}{x^3}\ln(x)^2 + \left(\frac{\Gamma_{\beta 1}}{x^3}+\frac{\Gamma_{\beta 2}}{x^5}\right)\ln(x) + \frac{\Gamma_\gamma}{x^3}+\frac{\Gamma_\delta}{x^5}+\frac{\Gamma_\varepsilon}{x^7}\right] \tag{14}$$

where

$$\Gamma_\alpha := -24(2\beta_2-\beta_1\alpha_1)\,\kappa^6(\kappa^2-1)^2 \tag{14a}$$

$$\Gamma_{\beta 1} := \left[\frac{(3\ln(\kappa)\,\kappa^2+3\ln(\kappa)-2\kappa^2+2)(-1)}{\ln(\kappa)}\beta_1^2-4\kappa^2\beta_1\alpha_1+8\kappa^2\beta_2\right] \times 12\ln(\kappa)\,\kappa^6(\kappa^2-1) \tag{14b}$$

$$\Gamma_{\beta 2} := -48\kappa^6(\beta_1^2+2\beta_2-\beta_1\alpha_1)\ln(\kappa)\,\kappa^2(\kappa^2-1) \tag{14c}$$

$$\Gamma_\gamma := (-2\beta_2+\alpha_1\beta_1)\,\Gamma_{\gamma 2}+\Gamma_{\gamma 1}\beta_1^2 \tag{14d}$$

$$\Gamma_{\gamma 1} := 4\kappa^6[(4\kappa^4+4\kappa^2-5)\ln(\kappa)^2 + 3(\kappa^2-1)(\kappa^2+3)\ln(\kappa)-3(\kappa^2-1)^2] \tag{14d.1}$$

$$\Gamma_{\gamma 2} := 2\kappa^6(\kappa^2-1)[(4+8\kappa^2)\ln(\kappa)^2+(9\kappa^2+9)\ln(\kappa)+6-6\kappa^2] \tag{14d.2}$$

$$\Gamma_\delta := -24\kappa^8\ln(\kappa)[(-\kappa^2+\ln(\kappa)\,\kappa^2+1+3\ln(\kappa))\,\beta_1^2 + 2\ln(\kappa)\,\kappa^2\alpha_1\beta_1-4\ln(\kappa)\,\kappa^2\beta_2] \tag{14e}$$

$$\Gamma_\varepsilon := -12\ln(\kappa)^2\,(4\beta_2+\beta_1^2-2\beta_1\alpha_1)\,\kappa^{10} \tag{14f}$$

Case II:

$$\gamma_0(x) = \frac{C_0}{x^3} \tag{15}$$

$$\gamma_1(x) := \left[\frac{-1}{2\kappa^2x^3}\ln(x)+\frac{1}{8}\frac{(2\kappa^2+\kappa^4-3-4\ln(\kappa))}{\kappa^2(\kappa^2-1)\,x^3}-\frac{1}{4x^5}\right] C_0^3\beta_1 \tag{16}$$

$$\gamma_2(x) := \left[U_\alpha\frac{\ln(x)^2}{x^3}+\left(\frac{U_\beta}{x^5}+\frac{U_\gamma}{x^3}\right)\ln(x)+\frac{U_\delta}{x^3}+\frac{U_\varepsilon}{x^5}-\frac{U_\zeta}{x^7}\right] C_0^5 \tag{17}$$

where

$$U_\alpha := \frac{-1}{8}\frac{(\beta_1\alpha_1 - 2\beta_2)}{\kappa^4} \tag{17a}$$

$$U_\beta := \frac{1}{8}\frac{(\beta_1^2 + 2\beta_2 - \beta_1\alpha_1)}{\kappa^2} \tag{17b}$$

$$U_\gamma := \frac{(8\ln(\kappa) + 4\ln(\kappa)\kappa^2 - 7\kappa^2 + 6 + \kappa^4)}{16(\kappa^2-1)\cdot\kappa^4}\beta_1^2 + \frac{1}{8\cdot\kappa^2}\alpha_1\beta_1 - \frac{1}{4\kappa^2}\beta_2 \tag{17c}$$

$$U_\delta := U_{\delta 1}\beta_1^2 + U_{\delta 2}(\alpha_1\beta_1 - 2\beta_2) \tag{17d}$$

$$U_{\delta 1} := \frac{1}{192}\frac{\begin{pmatrix}48(\kappa^2+2)\ln(\kappa)^2 - 48(\kappa^2-1)(\kappa^2+3)\ln(\kappa) \\ -(4\kappa^4 - 2\kappa^2 - 47)(\kappa^2-1)^2\end{pmatrix}}{(\kappa^2-1)^2\kappa^4} \tag{17d.1}$$

$$U_{\delta 2} := \frac{24\ln(\kappa)^2 + (36 - 24\kappa^2)\ln(\kappa) + (4\kappa^2+17)(\kappa^2-1)^2}{192\kappa^4(1-\kappa^2)} \tag{17d.2}$$

$$U_\varepsilon := \frac{1}{32}\frac{(-6\kappa^2 + \kappa^4 + 5 + 12\ln(\kappa))}{\kappa^2(\kappa^2-1)}\beta_1^2 + \frac{1}{16}\beta_1\alpha_1 - \frac{1}{8}\beta_2 \tag{17e}$$

$$U_\zeta := \frac{1}{64}(-4\beta_2 - \beta_1^2 + 2\beta_1\alpha_1) \tag{17f}$$

3. RESULTS AND DISCUSSION

3.1. Validation

To determine the range of validity of the series result for $\gamma_{r\theta}$, the boundary-value problem defined by Eqs. (1) and (2) is solved numerically, subject to the boundary conditions of Eqs. (8) and (9) and with material properties corresponding to Eqs. (4) and (5). Subroutine DMOLCH of the IMSL Library of Mathematical Software is used for this purpose. DMOLCH is a well-tested and benchmarked subroutine which applies the method of lines along with cubic Hermite interpolation polynomials to solve general systems of parabolic partial differential equations. The solution of Eqs. (1) and (2) is obtained as the steady-state result of the transient problem solved by DMOLCH. A linear dependence of k/k_0 (since α_1 is the only coefficient of the thermal conductivity model that affects the second-order result for velocity) and a quadratic of μ_0/μ on Θ has been

Table I. The Norm of the PRE Between Numerical and Series Solutions for the Shear Rate in a Circular Couette for a Range of Values of Br β_1 and κ: $\beta_1 = 1$, $\beta_2 = 0.5$, $\alpha_1 = 0.1$, $\alpha_2 = 0.0$ (Case I)

	$\kappa = 0.85$		$\kappa = 0.75$		$\kappa = 0.65$	
Br β_1	Norm(γ)	$\Delta\gamma_{max}$	Norm(γ)	$\Delta\gamma_{max}$	Norm(γ)	$\Delta\gamma_{max}$
1.5	0.032	0.169	0.021	0.112	0.013	0.068
3.0	0.252	1.34	0.168	0.892	0.103	0.541
4.0	0.586	3.15	0.393	2.09	0.242	1.28
5.0	1.12	6.08	0.754	4.05	0.466	2.48
6.0	1.89	10.4	1.28	6.93	0.794	4.25
7.0	—	—	—	—	1.24	6.69

considered in the numerical solution. The accuracy of the numerical algorithm has been verified separately through detailed comparison with analytical solution when $\alpha_1 = 0$ [9].

Tables I and II summarize the results of a comparison between numerical (based on a 400-node spatial discretization) and series solutions for the distribution of the shear rate across the gap of the Couette, for Cases I and II, respectively. Listed are the values of the norm of the percentage relative error (PRE), which is defined as

$$\text{norm}(\gamma_{r\theta}) = \frac{100}{K} \sum_{j=1}^{K} \frac{|\gamma_{r\theta,\,n} - \gamma_{r\theta,\,s}|_j}{|\gamma_{r\theta,\,n}|_j} \tag{18}$$

where the subscript j indicates the jth node across the gap, K is the total number of nodes, and the subscripts n and s indicate numerical and series solutions, respectively.

Table II. The Norm of the PRE Between Numerical and Series Solutions for the Shear Rate in a Circular Couette for a Range of Values of Br β_1 and κ: $\beta_1 = 1$, $\beta_2 = 0.5$, $\alpha_1 = 0.1$, $\alpha_2 = 0.0$ (Case II)

	$\kappa = 0.85$		$\kappa = 0.75$		$\kappa = 0.65$	
Br β_1	Norm(γ)	$\Delta\gamma_{max}$	Norm(γ)	$\Delta\gamma_{max}$	Norm(γ)	$\Delta\gamma_{max}$
0.5	0.11	0.55	0.09	0.45	0.08	0.36
0.75	0.36	1.83	0.31	1.51	0.26	1.18
1	0.83	4.24	0.73	3.53	0.60	2.76
1.25	1.58	8.21	1.38	6.78	1.15	5.30
1.5	2.66	13.9	2.33	11.5	1.94	9.01

For Case II and for the material parameters used, the accuracy of the series solution for the shear rate profile is satisfactory, with the norm of the errors being less than 1% for $\mathrm{Br}\,\beta_1$ up to about 1.2 (depending on κ). However, the maximum deviation between series and numerical solutions ($\Delta\gamma_{max}$) occurs at the location of the minimum shear rate (that is, on the surface of the rotating wall) and is higher than the average errors shown in Table II; for $\mathrm{Br}\,\beta_1 = 0.75$ the maximum relative error for the shear rate calculated from the series solution is 1.83%, while for $\mathrm{Br}\,\beta_1 = 1.5$ it is 13.9% (for $\kappa = 0.85$). Similar comments can be made for Case I (Table I), along with the observation that the range of validity of the series solution is in this case extended to $\mathrm{Br}\,\beta_1$ about 6 (again, depending on κ). It should be pointed out at this stage that quoting the Br alone is not sufficient to quantify the effect of viscous heating on the perturbed gapwise shear rate profile, since the deviation from simple shear flow depends not only on the extent of viscous heating (which is expressed by Br) but also on the sensitivity of the fluid viscosity on temperature (which is expressed by β). The appropriate scale in this case is the Nahme number [10]. For this reason, viscous heating is quantified by the use of the product $\mathrm{Br}\,\beta_1$ instead of Br alone in the following discussion. It is clear from Eq. (10) and Eqs. (12)–(17) that the derived expressions for $\gamma_{r\theta}$ can easily be formulated as expansions in terms of the product $\mathrm{Br}\,\beta_1$.

3.2. Shear Rate Distributions

For a fluid with temperature-dependent transport properties and for the boundary conditions of Case I, the effect of viscous heating is to reduce the shear rate on the inner and outer walls and thus cause the development of a local maximum in $\gamma_{r\theta}$ in the interior of the fluid. Figures 2a and b show the profiles of the normalized shear rate, calculated through the second-order series solution for a circular Couette with $\kappa = 0.5$, for two values of $\mathrm{Br}\,\beta_1$. The zeroth-order shear-rate profile, corresponding to isothermal flow (or to a fluid whose transport properties are temperature independent) is also shown, along with the shear rate profile derived from the first-order series solution. The agreement between the second-order solution and the numerical result is satisfactory for values of $\mathrm{Br}\,\beta_1$ up to about 8, with the highest discrepancy occurring on the surface of the inner cylinder. Increasing $\mathrm{Br}\,\beta_1$ results in a reduction of $\gamma_{r\theta}$ at the inner wall (compare Figs. 2a and b) and in the gradual development of a shear rate maximum at some location inside the fluid. Increasing κ results in a more pronounced maximum in $\gamma_{r\theta}$, which is shifting toward the middle of the gap, all other conditions being equal. This can be seen by comparing Figs. 3a and b, in which the distribution of $\gamma_{r\theta}$ in Couettes with $\kappa = 0.7$ and 0.8

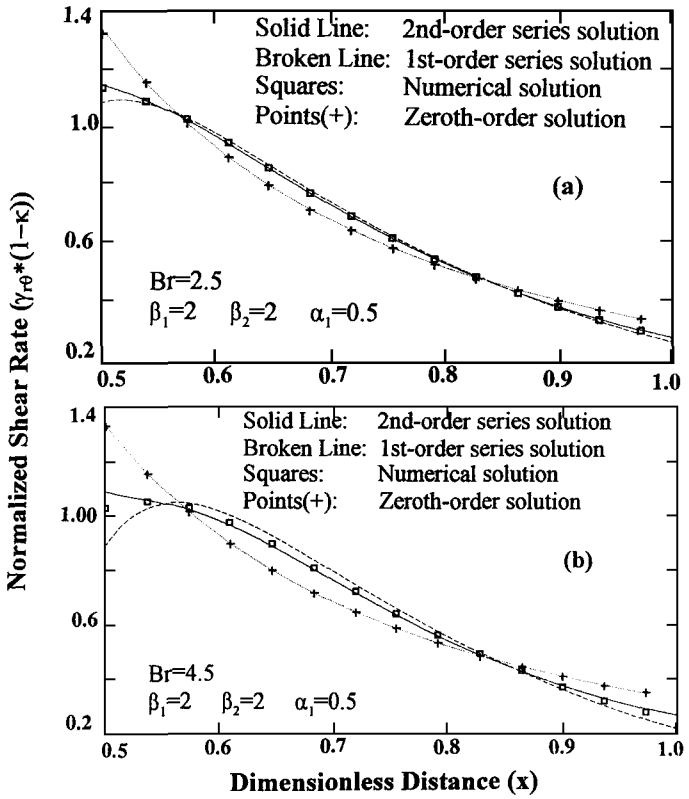

Fig. 2. Predictions of the series and of the numerical solutions for the shear rate profile in circular Couette flow ($\kappa = 0.5$) at two levels of the product Br β_1, namely, Br $\beta_1 = 5.0$ (a) and Br $\beta_1 = 9.0$ (b). Shown for comparison are the predictions of the first-and zeroth-order series solutions. Case I.

is shown, with Fig. 2a. It is evident that the distribution of shear rate is nonsymmetrical and that the inner cylinder surface is experiencing a higher shear rate than the surface of the outside cylinder. This is true even for κ as large as 0.95 (a value for which the flow in the Couette is usually considered to be planar). It is also evident that at higher values of κ and/or Br β_1, one has to gain from the extra accuracy of the second-order result for the shear rate.

For the boundary conditions corresponding to Case II, substantial viscous heating occurs at lower values of Br β_1 and the maximum temperatures are observed in the vicinity of the inner cylinder. As a result, the shear rate profile is monotonic, with the highest shear rate on the inner-cylinder wall and the lowest at the wall of the outside (rotating) cylinder.

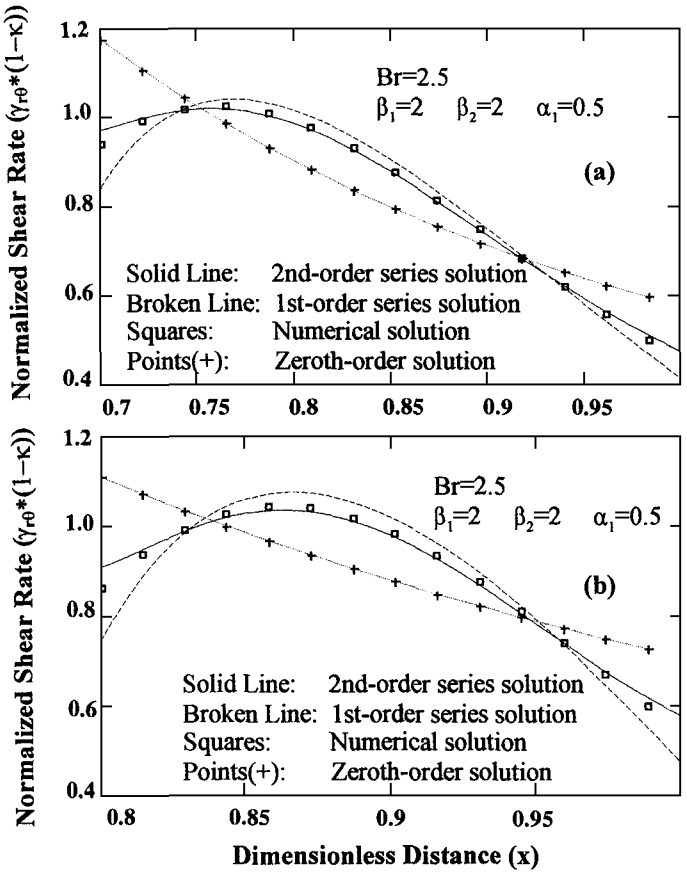

Fig. 3. Predictions of the series and of the numerical solutions for the shear rate profile in circular Couette flow at two levels of the parameter κ, namely, $\kappa = 0.7$ (a) and $\kappa = 0.8$ (b) and for Br $\beta_1 = 5.0$. Shown for comparison are the predictions of the first- and zeroth-order series solutions. Case I.

Increasing the value of the product Br β_1 makes this transition sharper, as can be seen in Figs. 4a and b, for the case of $\kappa = 0.625$. The effect of increasing the parameter κ is further shown in Figs. 5a and b.

3.3. Rheological Corrections in a Circular Couette Viscometer

The solutions for $\gamma_{r\theta}$ presented previously are now used to develop corrections for the interpretation of angular velocity vs torque data, such as those obtained during measurement of fluid viscosity through the use of

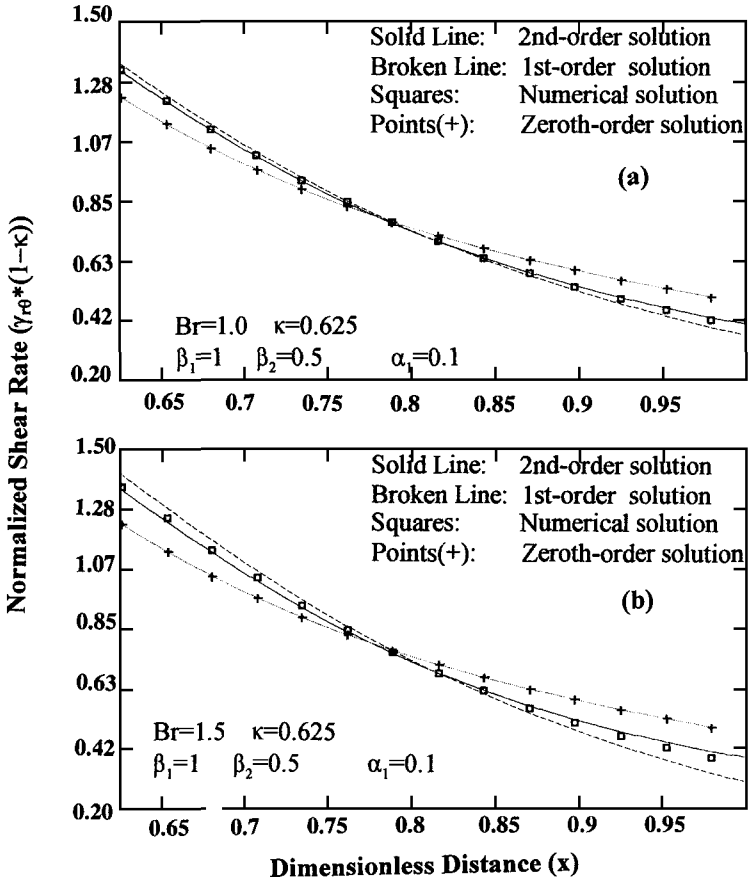

Fig. 4. Predictions of the series and of the numerical solutions for the shear rate profile in circular Couette flow ($\kappa = 0.625$) at two levels of the product $\mathrm{Br}\,\beta_1$, namely, $\mathrm{Br}\,\beta_1 = 1.0$ (a) and $\mathrm{Br}\,\beta_1 = 1.5$ (b). Shown for comparison are the predictions of the first- and zeroth-order series solutions. Case II.

the device described in Fig. 1, in cases where viscous heating and its effect on fluid properties are important. Elementary analysis shows that the torque, F, required to turn the outer cylinder of the viscometer is

$$F = 2\pi R^2 L \mu_0 (\gamma_{r\theta})_{r=R} \tag{19}$$

where L is the height of the cylinders and $(\gamma_{r\theta})_{r=R}$ is the shear rate at the inner surface of the rotating cylinder (given by expressions in previous section). Through Eq. (19), the viscosity of the fluid is found simply as the

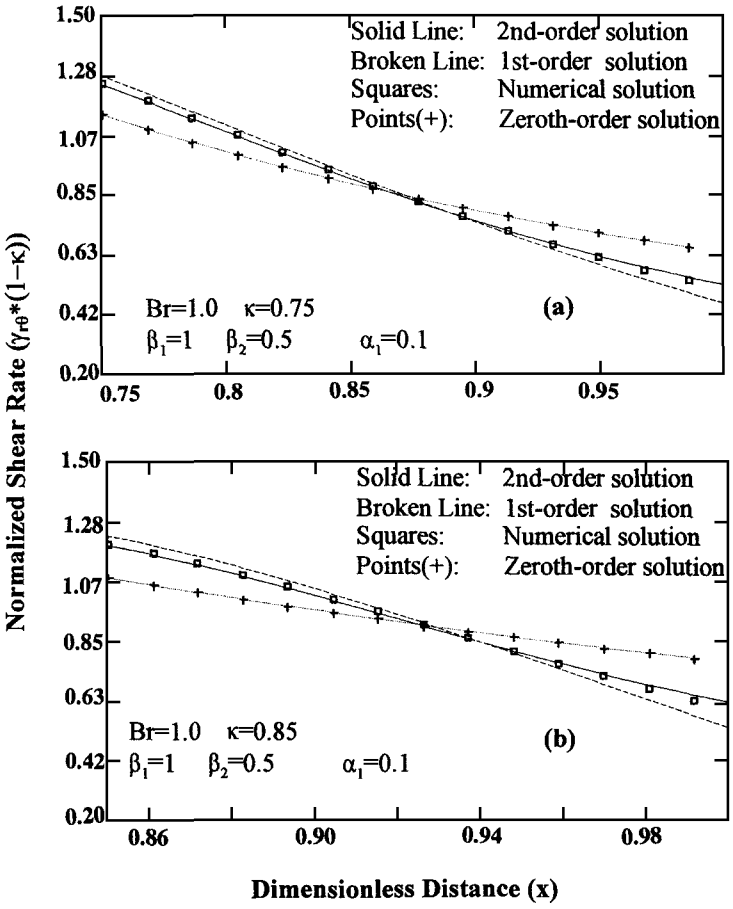

Fig. 5. Predictions of the series and of the numerical solutions for the shear rate profile in circular Couette flow at two levels of the parameter (κ), namely, $\kappa = 0.75$ (a) and $\kappa = 0.85$ (b) and for Br $\beta_1 = 1.0$. Shown for comparison are the predictions of the first- and zeroth-order series solutions. Case II.

ratio between the torque (measured experimentally) and the shear rate on the surface of the rotating cylinder. The latter can be calculated only when the velocity field in the viscometer is known. When this is not the case, the wall shear rate is calculated assuming an equivalent Newtonian fluid, in which case the viscosity obtained through Eq. (19) is an "apparent" viscosity that will coincide with the true viscosity of the fluid only in the absence of non-Newtonian or thermal effects. When such effects are present, the apparent viscosity needs to be *corrected* by accounting for the

actual velocity profile between the two cylinders. In the case of temperature-dependent transport properties in the presence of viscous heating, a solution for the shear rate profile has been presented in this work, and therefore, Eq. (19) can be rewritten as

$$F = 2\pi R^2 L \mu_0 \gamma_0 f^{(c)} \tag{20}$$

where $f^{(c)}$ is a correction term which accounts for the sensitivity of the transport properties of the fluid on temperature in the presence of viscous heating. This term can be expressed as

$$f^{(c)} = 1 + \mathrm{Br}\left(\frac{\gamma_1}{\gamma_0}\right) + \mathrm{Br}^2\left(\frac{\gamma_2}{\gamma_0}\right) \tag{21}$$

where the constants γ_0, γ_1, and γ_2 can be found from the results presented in previous section for $x = 1$ and are given below.

Case I:

$$\gamma_0 := \frac{2\kappa^2}{(1-\kappa^2)} \tag{22}$$

$$\gamma_1 := \beta_1 \kappa^4 \frac{(\kappa^2 \ln(\kappa) - \kappa^2 + \ln(\kappa) + 1)}{\ln(\kappa)(-1+\kappa^2)^3} \tag{23}$$

$$\gamma_2 := \frac{\kappa^6}{12(\kappa^2-1)^5 \ln(\kappa)^2} [\gamma_{2\alpha}\beta_1^2 + (2\beta_2 - \beta_1\alpha_1)\gamma_{2\beta}] \tag{24}$$

where the coefficients $\gamma_{2\alpha}(\kappa)$ and $\gamma_{2\beta}(\kappa)$ are given by

$$\begin{aligned}\gamma_{2\alpha}(\kappa) := {} & (-10\kappa^4 - 28\kappa^2 - 10)\ln(\kappa)^2 + 18(\kappa^4 - 1)\ln(\kappa) \\ & - 6\kappa^4 + 12\kappa^2 - 6\end{aligned} \tag{25}$$

$$\begin{aligned}\gamma_{2\beta}(\kappa) := {} & 4(\kappa^2 - \kappa + 1)(1 + \kappa + \kappa^2)\ln(\kappa)^2 \\ & - 9(\kappa^4 - 1)\ln(\kappa) + 6 + 6\kappa^4 - 12\kappa^2\end{aligned} \tag{26}$$

Case II:

$$\gamma_0 := \frac{2\kappa^2}{(1-\kappa^2)} \tag{27}$$

$$\gamma_1 := \frac{-1}{8} \frac{(-4\kappa^2 + \kappa^4 + 3 + 4\ln(\kappa))}{\kappa^2(-1+\kappa^2)} C_0^3 \beta_1 \tag{28}$$

$$\gamma_2 := [\gamma_{2\alpha}\beta_1^2 - \gamma_{2\beta}(-\alpha_1\beta_1 + 2\beta_2)]\, C_0^5 \tag{29}$$

where the coefficients $\gamma_{2\alpha}(\kappa)$ and $\gamma_{2\beta}(\kappa)$ are given by

$$\gamma_{2\alpha}(\kappa) := \frac{\begin{pmatrix} 48(\kappa^2+2)\ln(\kappa)^2 + 24(\kappa^2-1)(\kappa^2-6)\ln(\kappa) \\ +(5\kappa^4-28\kappa^2+47)(\kappa^2-1)^2 \end{pmatrix}}{(-1+\kappa^2)^2\,192\kappa^4} \tag{30}$$

$$\gamma_{2\beta}(\kappa) := \frac{-24\ln(\kappa)^2 + 12(2\kappa^2-3)\ln(\kappa) + (\kappa^2-1)(2\kappa^4-13\kappa^2+17)}{192\kappa^4(-1+\kappa^2)} \tag{30a}$$

For the case of isothermal walls (Case (I)), a second-order in Br series solution in the case of planar Couette flow ($\kappa=1$) has been derived in Ref. 1. From this solution, it can be shown that

$$f^{(c)}_{(\kappa=1)} = 1 - \frac{\beta_1}{12}\,\mathrm{Br} + \left(\frac{\beta_1^2}{80} - \frac{\beta_2}{120} + \frac{\beta_1\alpha_1}{240}\right)\mathrm{Br}^2 \tag{31}$$

Taking formal limits of the expressions for $\gamma_0 - \gamma_2$ corresponding to isothermal walls [Eqs. (22)–(24)], it can be shown that

$$\lim_{\kappa\to 1}\left(\frac{\gamma_2}{\gamma_0}\right) = \frac{\beta_1^2}{80} - \frac{\beta_2}{120} + \frac{\beta_1\alpha_1}{240} \qquad \text{and} \qquad \lim_{\kappa\to 1}\left(\frac{\gamma_1}{\gamma_0}\right) = -\frac{\beta_1}{12} \tag{32}$$

Therefore, the derived expressions for $f^{(c)}$ in the case of circular Couette flow collapse to the result obtained for simple-shear flow, when κ approaches unity.

For Case II, the velocity profile in planar Couette flow, up to second order in Br, has been derived in this work and is

$$u_0(\xi) = \xi \tag{33}$$

$$u_1(\xi) := \tfrac{-1}{6}\beta_1\xi^3 + \tfrac{1}{6}\beta_1\xi \tag{34}$$

$$u_2(\xi) := (\tfrac{1}{20}\beta_2 - \tfrac{1}{40}\beta_1\alpha_1 + \tfrac{1}{120}\beta_1^2)\,\xi^5 + (\tfrac{1}{12}\beta_1^2 + \tfrac{1}{12}\beta_1\alpha_1 - \tfrac{1}{6}\beta_2)\,\xi^3 \ldots + (\tfrac{-7}{120}\beta_1\alpha_1 - \tfrac{11}{120}\beta_1^2 + \tfrac{7}{60}\beta_2)\,\xi \tag{35}$$

where ξ is the corresponding planar coordinate, which varies between zero (adiabatic, stationary wall) and one (rotating, isothermal wall). From the above result, it can be shown that the correction term in the limit of planar flow ($\kappa \to 1$) is

$$f^{(c)}_{(\kappa=1)} = 1 - \frac{\beta_1}{3}\,\mathrm{Br} + \left(\frac{\beta_1^2}{5} - \frac{2\beta_2}{15} + \frac{\beta_1\alpha_1}{15}\right)\mathrm{Br}^2 \tag{36}$$

As in Case I, it can be shown that the results for $\gamma_0 - \gamma_2$ obtained for Case II [Eqs. (27)–(30)] satisfy

$$\lim_{\kappa \to 1} \left(\frac{\gamma_2}{\gamma_0} \right) = \frac{\beta_1^2}{5} - \frac{2\beta_2}{15} + \frac{\beta_1 \alpha_1}{15} \qquad \text{and} \qquad \lim_{\kappa \to 1} \left(\frac{\gamma_1}{\gamma_0} \right) = -\frac{\beta_1}{3} \tag{37}$$

and are thus asymptotically correct.

The correction term $f^{(c)}$ for Case I is plotted in Fig. 6 as a function of the product $\mathrm{Br}\,\beta_1$, for five values of the geometrical parameter κ. The limiting result as κ approaches unity [Eq. (31)] is also shown as a solid line for comparison. It can be seen that for $\kappa > 0.9$, the result of Ref. 1 is applicable; at lower values of the eccentricity parameter κ, the results derived in this study should be used instead. The correction term corresponding to Case II is shown in Fig. 7 as a function of $\mathrm{Br}\,\beta_1$ for a range of values of the eccentricity parameter κ. As in Fig. 6, the result corresponding to planar Couette flow is shown as a solid line for comparison. In both Fig. 6 and Fig. 7 it can be seen that for small values of $\mathrm{Br}\,\beta_1$ (that is, for small Br or for a fluid with almost constant viscosity), the correction term approaches the limiting value of 1. As the value of the product $\mathrm{Br}\,\beta_1$ increases, the correction term deviates from unity; this deviation occurs earlier (at lower values of $\mathrm{Br}\,\beta_1$) for higher values of κ. Another observation is that the correction term in the adiabatic case starts deviating from unity at lower values of $\mathrm{Br}\,\beta_1$ as compared to the $f^{(c)}$ obtained for Case I. In the former case, for $\mathrm{Br}\,\beta_1$ as low as 0.1, the correction term is already about around 0.96–0.97, while in the latter it is still roughly unity. The obtained correction factors extend to about 0.8 for both cases; the solution for Case I is valid for a wider range of $\mathrm{Br}\,\beta_1$ compared to Case II. The local minima observed in some of the curves in Figs. 6 and 7 have no physical meaning and simply indicate that the second-order series solution is no longer valid at the corresponding values of $\mathrm{Br}\,\beta_1$. Similar behavior has been seen in the results of Ref. 1 for the correction term in cone-and-plate viscometers.

The sensitivity of the correction term for Case I [Eqs. (22)–(24)] on the transport properties of the fluid is summarized in the contour graph in Fig. 8. Plotted is the correction term $f^{(c)}$ as a function of α_1 ($-1.0 < \alpha_1 < 1.0$) and $\beta_1(0; 0 < \beta_1 < 2.0)$. When β_1 is small, the predicted correction term is largely independent of α_1 (and approaches unity as β_1 approaches zero) regardless of the specific value of the latter, as evidenced by contour lines running almost parallel to the α_1-axis. This simply expresses the fact that for a material with temperature-insensitive viscosity (small β_1), the ease by which heat is conducted in it has only a minimal effect on Couette measurements. For large β_1, that is, for viscosity strongly dependent on

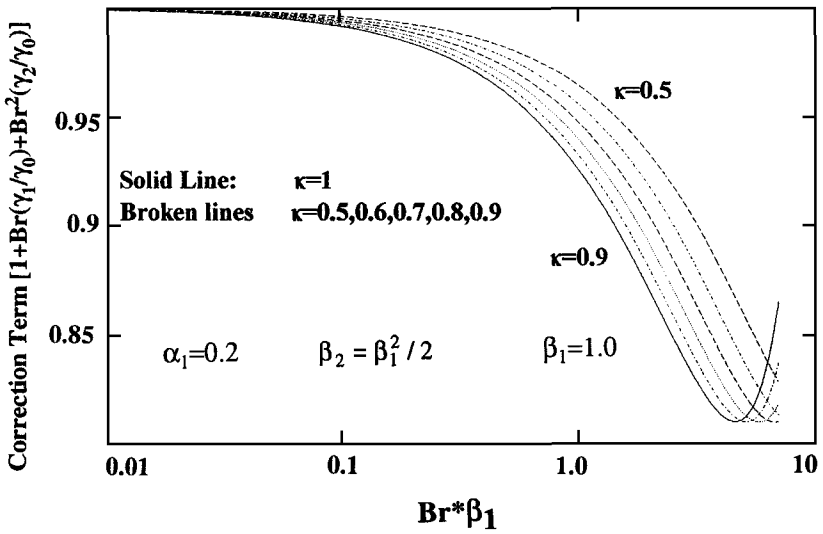

Fig. 6. The effect of the parameter Br β_1 in a Couette–Hatschek viscometer on the value of the correction term [Eqs. (22)–(24)] for five values on the geometrical parameter (κ). The result corresponding to planar flow [Eq. (31)] is shown as a solid line. Case I.

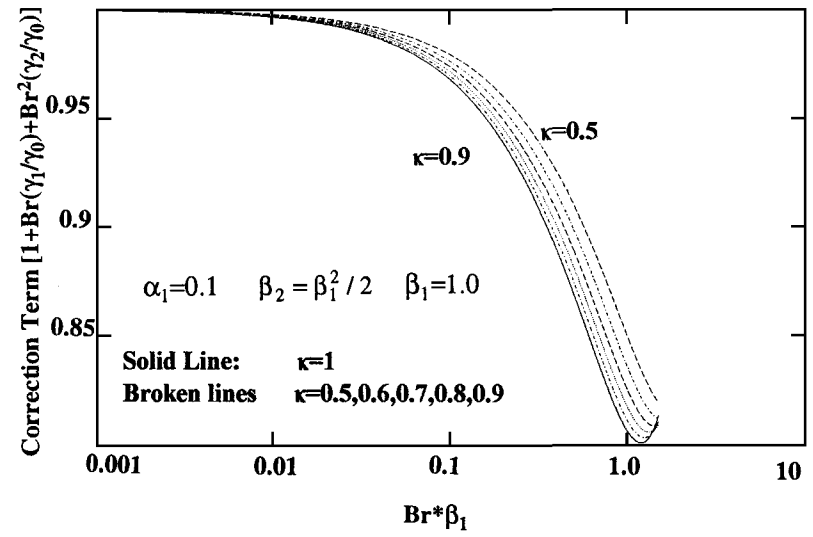

Fig. 7. The effect of Br β_1 in a Couette–Hatschek viscometer on the value of the correction term [Eqs. (21) and (27)–(29)] for five values on the geometrical parameter (κ). The result corresponding to planar flow [Eq. (36)] is shown as a solid line. Case II.

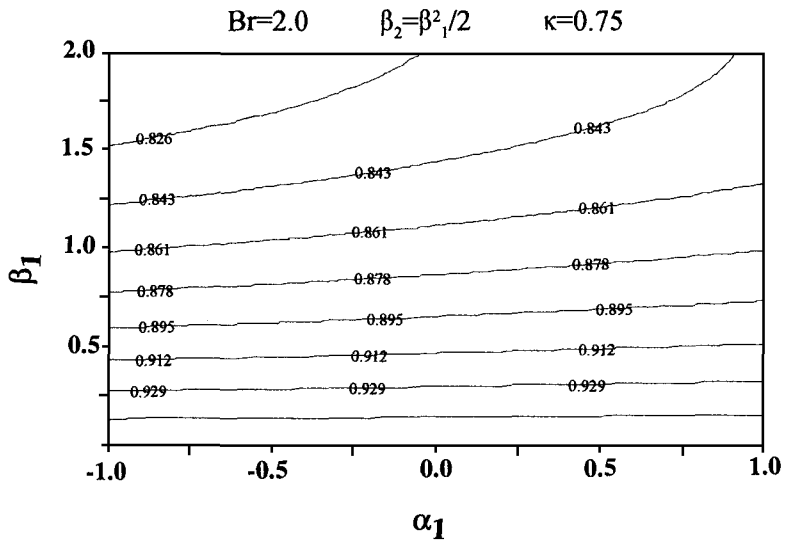

Fig. 8. The sensitivity of the correction term for a Couette–Hatschek viscometer in Case I [Eqs. (22)–(24)] on the material parameters α_1 and β_1.

temperature, a temperature-dependent thermal conductivity (k) affects the value of the correction term; when k increases with temperature ($\alpha_1 > 0$) the value of the correction term increases toward unity with increasing α_1 [that is, the effect of a viscosity decreasing sharply with temperature (large β_1) is "balanced" by a more conductive fluid which facilitates the removal of the generated heat]. The opposite is true when β_1 is large and $\alpha_1 < 0$ (thermal conductivity decreasing with increasing temperature), in which case the value of the correction term deviates from unity with increasing $|\alpha_1|$.

4. CONCLUSION

Series solutions, up to second order in the Brinkman number, have been developed for the distribution of shear rate in circular Couette flow of materials whose viscosity and thermal conductivity can be expressed as polynomial functions of temperature with arbitrary coefficients. Both isothermal and mixed boundary conditions have been considered. The derived solutions have been validated by extensive comparison to numerical solutions and are found to be reliable for a practical range of $\mathrm{Br}\,\beta_1$. Formal corrections for viscosity measurements in circular Couette viscometers, which account for viscous heating and temperature-dependent transport

properties, are derived and are shown to exhibit the anticipated asymptotic behavior in the limit of planar flow. Viscous heating, expressed by the product $\mathrm{Br}\,\beta_1$, is found to affect the correction term more profoundly in the case of an adiabatic inner (stationary) cylinder. In both cases, the correction term is reliable down to a value about 0.8. The sensitivity of the derived correction formulae on material (α_i, β_i) and process (Br) parameters has also been investigated.

REFERENCES

1. R. M. Turian, and R. B. Bird, *Chem. Eng. Sci.* **18**:689 (1963).
2. R. M. Turian, *Chem. Eng. Sci.* **20**:771 (1965).
3. K. A. Caridis, B. Louwagie, and T. D. Papathanasiou, *J. Chem. Eng. Japan* **30**(1):123–136 (1997).
4. T. D. Papathanasiou, K. A. Caridis, and B. Bjeljic, *Int. J. Thermophys.* **18**:125 (1997).
5. R. J. Phillips, R. C. Armstrong, R. A. Brown, A. L. Graham, and J. R. Abbott, *Phys. Fluids A* **4**:30 (1992).
6. H. M. Laun, R. Bung, S. Hess, W. Loose, O. Hess, K. Hahn, E. Hadicke, R. Hingmann, F. Schmidt, and P. Lindner, *J. Rheol.* **36**(4):743 (1992).
7. A. W. Chow, S. W. Sinton, and J. H. Iwamiya, *Mater. Res. Soc. Symp. Proc.* **289**:95 (1993).
8. R. B. Bird, W. E. Stewart, and E. N. Lightfoot, *Transport Phenomena* (Wiley, New York, 1960).
9. J. Gavis and R. L. Lawrence, *I&EC Fund.* **7**(2):232 (1968).
10. J. R. A. Pearson, *Mechanics of Polymer Processing* (Elsevier, London, 1985).